

Simulation and theory of fluid demixing and interfacial tension of mixtures of colloids and nonideal polymers

R. L. C. Vink

Institut für Physik, Johannes-Gutenberg-Universität, Staudinger Weg 7, D-55099 Mainz, Germany

Matthias Schmidt*

Soft Condensed Matter, Debye Institute, Utrecht University, Princetonplein 5, 3584 CC Utrecht, The Netherlands

(Received 4 January 2005; published 31 May 2005)

An extension of the Asakura-Oosawa-Vrij model of hard sphere colloids and nonadsorbing polymers is studied with grand canonical Monte Carlo simulations and density functional theory. Polymer nonideality is taken into account through a repulsive step-function pair potential between polymers. Simulation results validate previous theoretical findings for the shift of the bulk fluid demixing binodal upon increasing strength of polymer-polymer repulsion, indicating suppression of phase separation. For increasing strength of the polymer-polymer repulsion, simulation and theory consistently predict the interfacial tension of the free interface between the colloidal liquid and the colloidal gas phase to decrease significantly for fixed colloid density difference in the coexisting phases, and to increase for fixed polymer reservoir packing fraction.

DOI: 10.1103/PhysRevE.71.051406

PACS number(s): 82.70.Dd, 61.20.Ja, 64.75.+g, 61.20.Gy

I. INTRODUCTION

Various different levels of description have been employed in order to study mixtures of colloidal particles and nonadsorbing globular polymers [1,2]. While colloid-colloid interactions are reasonably well described by those of hard spheres, the effective interactions between colloids and polymers, as well as that between the centers of two polymers, are more delicate. The model due to Asakura and Oosawa [3] and Vrij [4] (AOV), taking the colloids to be hard spheres and the polymer-polymer interactions to vanish, is arguably the most simple description of real colloid-polymer mixtures. Its appeal clearly lies in its simplicity, rather than in very close resemblance of experimental colloid-polymer systems, enabling detailed simulation [5–9] and theoretical [6,10–13] studies of bulk [5–8] and interfacial [9,14–19] properties. More realistic effective interactions between the constituent particles can be systematically obtained by starting at the polymer segment level, and integrating out the microscopic degrees of freedom of the polymers [8,20]. The resulting colloid-polymer interaction is a smoothly varying function of distance, and excluded volume between polymer segments leads to a soft Gaussian-like polymer-polymer repulsion. Such effective interactions have been used to calculate bulk phase behavior [8,21,22].

In order to retain most of the simplicity of the AOV model, but still to capture polymer nonideality [23,24], the AOV model was extended using a repulsive step-function pair potential between polymers in Ref. [25] (note that using a pairwise potential is an approximation; for a study of realistic effective pair potentials for polymer solutions see, e.g., Ref. [26]). The colloid-polymer interaction was kept as that

of hard spheres. This introduces one additional model parameter, namely the ratio of step-height and thermal energy, interpolating between the AOV case when this quantity vanishes, and the additive binary hard sphere mixture when it becomes infinite. Following the hard sphere [27] and AOV cases [12,13], the well-defined particle shapes of this model allowed to obtain a geometry-based density functional theory (DFT) [28,29] specifically tailored for this model [25]. The theory can, in principle, be applied to arbitrary inhomogeneous situations, which constitutes an *a posteriori* justification for using these model interactions. The trends found for the fluid-fluid demixing transition into a colloidal liquid phase (that is rich in colloids and poor in polymers) and a colloidal gas phase (that is poor in colloids and rich in polymers), upon increasing the polymer-polymer interaction strength, demonstrated improved accordance with the experimental findings of Ref. [30], as compared to the AOV case [17,25], where the DFT predicts the same phase diagram as the free volume theory [11]. Furthermore the extended AOV model was used in the study of the “floating liquid phase” that was found in sedimentation-diffusion equilibrium [31]. Further discussion of the model and its relation to the AOV prescription is given in Ref. [25].

The aim of the present paper is twofold. First, we want to assess in detail the accuracy of the DFT of Ref. [25] by comparing to results from direct simulations of the extended AOV model. While phase coexistence is often studied in the Gibbs ensemble [32], we instead choose to take advantage of recently developed methods [7,33] that rely on the grand canonical ensemble. Benefits are accurate estimates of the interfacial tension [7,34] and access to the critical region [35]. The binodal we obtain in the simulations is compared to that from DFT, and good agreement between both is found. This result strongly supports the original claim that a straightforward perturbation theory, taking the AOV system as the reference state and adding polymer-polymer interactions in a mean-field-like manner, will fail, as the bulk fluid-

*Present address: Institut für Theoretische Physik II, Heinrich-Heine-Universität Düsseldorf, Universitätsstraße 1, D-40225 Düsseldorf, Germany.

fluid binodal from this approach differs markedly from that of the geometry-based DFT, as discussed in detail in Ref. [25]. Instead, even to lowest order in strength of the polymer-polymer interaction, a non-trivial coupling to the colloid density field needs to be taken into account; the DFT of Ref. [25] does this intrinsically. Our second aim is to study the interfacial tension between demixed colloidal gas and liquid phases, which is known from experiments [36–39], theory [14,16,17,40], and simulation [7,41] to be orders of magnitude smaller than that of atomic substances. While much work has been devoted to the case of noninteracting polymers [7,14,16–19,40,41], only quite recent studies addressed the effect of polymer nonideality [42–44]. Aarts *et al.* [42] use a square gradient approach based on the free energy of a free volume theory, to include polymer interactions [45], and the mean spherical approximation for the direct correlation function. They find the gas-liquid interfacial tension to decrease as compared to the case of noninteracting polymers, when plotted as a function of the density difference in the coexisting phases. Similar findings were reported by Moncho-Jordá *et al.* [43], who also used a square gradient approach, but based on an effective colloid-colloid depletion potential that reproduces simulation results accurately [46]. Our present study goes beyond Refs. [42,43], and also beyond the very recent Ref. [44] using perturbative DFT, as we employ a nonperturbative DFT treating the full two-component mixture of colloids and interacting polymers. We compare results for the interfacial tension to our data from direct simulation of the binary mixture. Besides its intrinsic interest, the interfacial tension is relevant for the occurrence of capillary condensation in confined systems [47–49] as is apparent from a treatment based on the Kelvin equation [50]. It determines static and dynamic properties of thermally excited capillary waves that decorate the interface; colloid-polymer mixtures are a primary model system to study capillary-wave induced roughness of interfaces [49,51]. We find good agreement of theoretical and simulation results demonstrating that the theory is well suited to tackle further interesting inhomogeneous situations of colloid-polymer mixtures under external influence.

The paper is organized as follows. In Sec. II we define the extended AOV model taking into account polymer-polymer repulsion. In Sec. III we briefly sketch the theoretical and simulation techniques. In Sec. IV results for fluid-fluid phase behavior and the interfacial tension are presented, and we conclude in Sec. V.

II. MODEL

We consider a mixture of hard sphere colloids (species c) of diameter σ_c , and effective polymer spheres (species p) of diameter σ_p , that interact via pairwise potentials $V_{ij}(r)$ with $(i,j) \in (c,p)$, as function of the center-to-center distance r between two particles, given as

$$V_{cc}(r) = \begin{cases} \infty & r < \sigma_c, \\ 0 & \text{otherwise,} \end{cases} \quad (1)$$

$$V_{cp}(r) = \begin{cases} \infty & r < (\sigma_c + \sigma_p)/2, \\ 0 & \text{otherwise,} \end{cases} \quad (2)$$

$$V_{pp}(r) = \begin{cases} \epsilon & r < \sigma_p, \\ 0 & \text{otherwise.} \end{cases} \quad (3)$$

Particle numbers are denoted by N_i , and as bulk thermodynamic parameters we use the packing fractions $\eta_i = \pi\sigma_i^3 N_i / (6V)$, where V is the system volume, and $i=c,p$. As an alternative to η_p , we use the packing fraction $\eta_p^f = \pi\sigma_p^3 \rho_p^f / 6$ in a reservoir of pure polymers, interacting via $V_{pp}(r)$ as given above, that is in chemical equilibrium with the system, with ρ_p^f being the polymer number density in the reservoir.

The model is characterized by two dimensionless control parameters, namely the polymer-to-colloid size ratio $q = \sigma_p / \sigma_c$, and the scaled strength of polymer-polymer repulsion, $\beta\epsilon$, with $\beta = 1/(k_B T)$, k_B the Boltzmann constant, and T the absolute temperature. As limiting cases, the present model possesses the AOV model for $\beta\epsilon=0$, where polymer-polymer interactions are ideal, and the binary additive hard sphere mixture in the limit $\beta\epsilon \rightarrow \infty$. One can use the parameter $\beta\epsilon$ to match to a real system at a given thermodynamic statepoint, polymer type and solvent, by imposing equality of the second (polymer-polymer) virial coefficients. See Ref. [25] for an in-depth discussion of this procedure.

It is to be noted that changing temperature in an experimental colloid-polymer mixture simultaneously affects the strength of polymer-polymer repulsion, $\beta\epsilon$, as well as the polymer size through coil swelling; see, e.g., Refs. [23,24] for thorough discussions, and Ref. [25] for the relation to the present model. In the presentation of our data we will follow a slightly artificial, but theoretically appealing, route of varying $\beta\epsilon$ at *constant* size ratio q .

III. METHODS

A. Density functional theory

To investigate bulk and interfacial properties of the present model, we use the geometrically based DFT of Ref. [25] that has its roots in generalizations of Rosenfeld's fundamental-measure theory for additive hard sphere mixtures [27], namely the treatment of the “penetrable sphere model” [52] (equivalent to the present polymer particles) and the DFT genuinely developed for the AOV model [12]. The minimization of the grand potential is carried out with a simple iteration technique. We refer the reader directly to Ref. [25] for all details about the (approximate) Helmholtz free energy functional.

B. Simulation method

The simulations are carried out in the grand canonical ensemble, where the fugacities z_c and z_p , of colloids and polymers, respectively, and the total volume V are fixed, while the number of particles, N_c and N_p , are allowed to fluctuate. We use a rectangular box of dimensions $L \times L \times D$, with periodic boundary conditions in all three spatial directions, and simulate the full mixture as defined by the pair potentials given in Eqs. (1)–(3), i.e., the positional degrees of freedom of both colloids and polymers are explicitly taken into account. Note that *asymmetric* binary mixtures are

in general difficult to simulate, and prone to long equilibration times. To alleviate this problem, we rely on a recently developed cluster move [7,53], that has already been applied successfully to the standard AOV model [7,35,53,54]. Here we perform the generalization to $\beta\epsilon > 0$ which is straightforward.

During the simulation, we measure the probability $P(\eta_c)$ of finding a certain colloid packing fraction η_c . At phase coexistence, the distribution $P(\eta_c)$ becomes bimodal, with two peaks of equal area, one located at small values of η_c corresponding to the colloidal gas phase, and one located at high values of η_c corresponding to the colloidal liquid phase. Typical coexistence distributions for the standard AOV model can be found in Ref. [7], and our present results display similar behavior. The equal area rule [55] implies that $\int_0^{\langle \eta_c \rangle} P(\eta_c) d\eta_c = \int_{\langle \eta_c \rangle}^{\infty} P(\eta_c) d\eta_c$, with $\langle \eta_c \rangle$ the average of the full distribution $\langle \eta_c \rangle = \int_0^{\infty} \eta_c P(\eta_c) d\eta_c$, where we assume that $P(\eta_c)$ has been normalized to unity $\int_0^{\infty} P(\eta_c) d\eta_c = 1$. The packing fraction of the colloidal gas, η_c^g , now follows trivially from the average of $P(\eta_c)$ in the first peak: $\eta_c^g = 2 \int_0^{\langle \eta_c \rangle} \eta_c P(\eta_c) d\eta_c$, and similarly for the colloidal liquid: $\eta_c^l = 2 \int_{\langle \eta_c \rangle}^{\infty} \eta_c P(\eta_c) d\eta_c$, where the factors of 2 are a consequence of the normalization of $P(\eta_c)$.

The interfacial tension γ is extracted from the logarithm of the probability distribution $W \equiv k_B T \ln P(\eta_c)$. Note that $-W$ corresponds to the free energy of the system. Therefore, the height F_L of the peaks in W , measured with respect to the minimum in between the peaks, equals the free energy barrier separating the colloidal gas from the colloidal liquid [34]. F_L may be related to the interfacial tension γ by noting that, at colloid packing fractions between the peaks $\eta_c^g \ll \eta_c \ll \eta_c^l$, the system consists of a colloidal liquid in coexistence with its vapor. A snapshot of the system in this regime reveals a so-called slab geometry, with one region dense in colloids, and one region poor in colloids, separated by an interface. (Because of periodic boundary conditions, two such interfaces are actually present.) If an elongated simulation box with $D > L$ is used, rather than a cubic box with $D = L$, the interfaces will be oriented perpendicular to the elongated direction, since this minimizes the interfacial area, and hence the free energy of the system. The total interfacial area in the system thus equals $2L^2$ and, following Ref. [34], $\gamma = F_L / (2L^2)$. An additional advantage of using an elongated simulation box is that interactions between the two interfaces are suppressed. This enhances a flat region in W between the peaks, which is required for an accurate estimate of the interfacial tension. In this work, an elongated box of dimensions $D/\sigma_c = 16.7$ and $L/\sigma_c = 8.3$ is used.

Close to the critical point the simulation moves back and forth easily between the gas and liquid phases, while further away from the critical point, i.e., at higher polymer fugacity, the free energy barrier between the two phases increases. Hence transitions from one to the other phase become less likely, and the simulation spends most of the time in only one of the two phases. A crucial ingredient in our simulation is therefore the use of a biased sampling technique. We employ successive umbrella sampling, as was recently developed by Virnau and Müller [33], to enable accurate sampling in regions of η_c where $P(\eta_c)$, due to the free energy barrier separ-

ating the phases, is very small. In this approach, states (or windows) are sampled successively. In the first window, the number of colloids is allowed to vary between 0 and 1, in the second window between 1 and 2, and so forth. The number of polymers is allowed to fluctuate freely in each window. Our sampling scheme is thus strictly one-dimensional: the bias is put on the colloid density only. Note that this becomes problematic for very large systems because of droplet formation. An additional free energy barrier, which grows with the size of the simulation box, must be crossed before the transition from the droplet state, to the slab geometry occurs (which is required if the interfacial tension is to be determined). As pointed out in Refs. [56,57], this additional barrier is not one in colloid density, but rather in the energylike parameter, which for our system would be the polymer density. Hence, for very large systems, a naive one-dimensional biasing scheme such as described above, is prone to severe sampling difficulties (more appropriate in this case would be a two-dimensional sampling scheme in both the colloid and the polymer density). For the system size used in the present study, however, no problems in obtaining the slab geometry were encountered.

In this work, we simulate up to a colloid packing fraction of $\eta_c \approx 0.45$, corresponding to a maximum of around 1000 colloidal particles. The maximum number of polymers is obtained at low η_c . While the precise number depends on η_p^f and $\beta\epsilon$, a value of 3000 is typical. In each window, $O(10^7)$ grand canonical cluster moves are attempted, of which $O(10^5)$ are accepted at low η_c , and $O(10^3)$ at high η_c (the grand canonical cluster move thus becomes less efficient with increasing colloid packing fraction). The typical CPU time investment to obtain a single distribution $P(\eta_c)$ is 48 hours on a moderate computer.

IV. RESULTS

In Fig. 1 we plot results for the bulk fluid-fluid demixing binodal as obtained from theory and simulation in the (η_c, η_p) plane, i.e., using the ‘‘system representation.’’ For the AOV case (recovered for $\beta\epsilon = 0$), the DFT predicts the same bulk free energy for fluid states, and hence the same demixing binodal, as free volume theory [11]. The theoretical binodal is known to compare overall reasonably well with simulation results for a variety of size ratios q , but to deviate from simulation results close to the critical point [5,7–9]. For increasing strength of the polymer-polymer repulsion, $\beta\epsilon$, (and constant size ratio q , i.e., neglecting impact on the polymer size upon changing temperature [23,24]) the theoretical critical point shifts toward higher values of η_c , and very slightly to lower values of η_p . The accompanying shift of the binodal leads to a growth of the one-fluid region in the phase diagram, hence polymer-polymer repulsion tends to promote mixing. The simulation results indicate the same trend, but show a quantitatively larger shift of the binodal toward higher values of η_c upon increasing $\beta\epsilon$. Note also the pronounced finite-size deviations of the simulation data in the vicinity of the critical point. As a result, the slight decrease in the critical value of η_p with increasing $\beta\epsilon$, as predicted by DFT, cannot be identified in the simulation data. To better

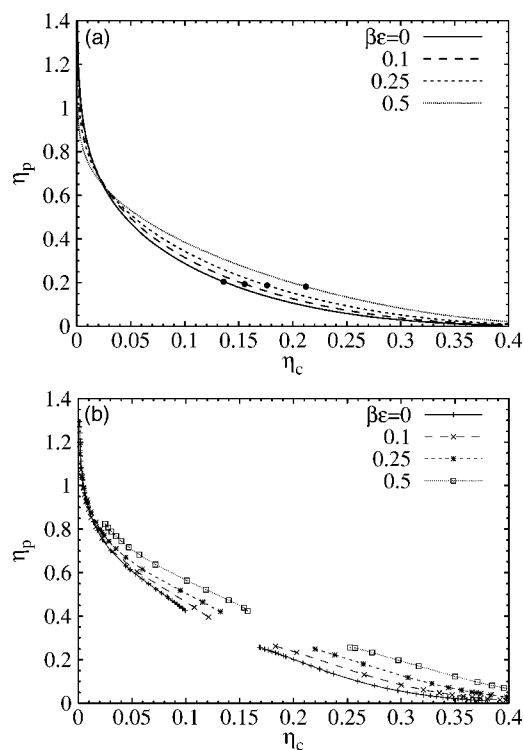


FIG. 1. Bulk fluid-fluid demixing phase diagram as a function of colloid packing fraction, η_c , and polymer packing fraction, η_p , for size ratio $q=0.8$ and increasing strength of the polymer-polymer repulsion $\beta\epsilon=0, 0.1, 0.25$, and 0.5 (as indicated). (a) The binodal (lines) and critical point (symbols) as obtained from DFT. The case $\beta\epsilon=0$ (dashed line and open symbol) corresponds to the result from free volume theory for the AOV model. (b) The binodal as obtained from simulations (symbols indicate data points; lines are guides to the eye).

access the critical region, a finite size scaling analysis [58–60] would be required. While such an investigation has been carried out for the standard AOV model [35], it would require extensive additional simulations for the extended model, which is beyond the scope of the present work.

When plotted in the (η_c, η_p^r) plane or “reservoir representation,” the theoretical results display a similar shift of the binodal toward larger values of η_c , and considerable broadening of the coexistence region; see Fig. 2. This implies that at a given value of η_p^r above the critical point, increasing the polymer-polymer repulsion leads to a larger density difference between the coexisting phases. The broadening of the coexistence region is strikingly confirmed by the simulation data. We again observe an overall shift of the binodals toward higher values of η_c . In accordance with findings for the standard AOV model [5,7–9], the critical value of η_p^r obtained by DFT underestimates the simulation value. This is related to the universality class of the AOV model, which is that of the 3D Ising model [35], and hence, close to criticality, deviations from a mean-field treatment like the present DFT are to be expected.

Increasing $\beta\epsilon$ has a profound impact on the range of values of the (scaled) chemical potential of polymers, $\beta\mu_p = \ln(z_p\sigma_p^3)$, at colloidal liquid-gas coexistence. We plot in Fig. 3 the phase diagram as a function of η_c and $\beta\mu_p$. A profound

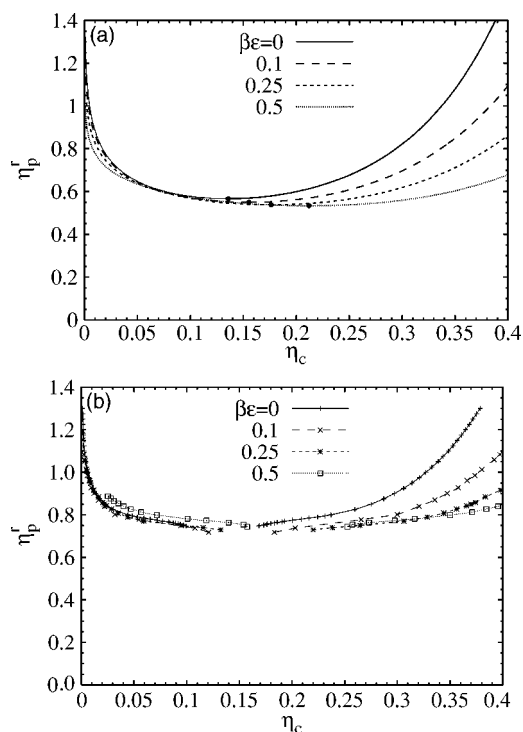


FIG. 2. The analog of Fig. 1, but as a function of colloid packing fraction, η_c , and polymer reservoir packing fraction, η_p^r , in a reservoir of interacting polymers. (a) DFT results; (b) simulation results.

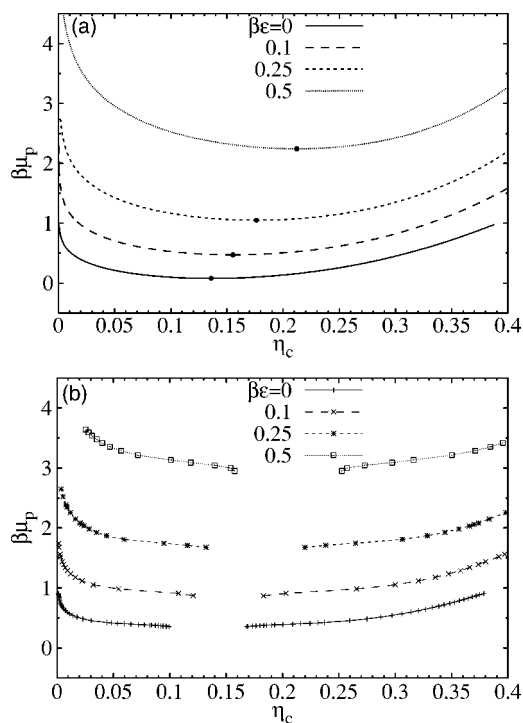


FIG. 3. The same as Fig. 1, but as a function of colloid packing fraction, η_c , and (scaled) chemical potential of polymers, $\beta\mu_p = \ln(z_p\sigma_p^3)$. (a) DFT results; (b) simulation results.

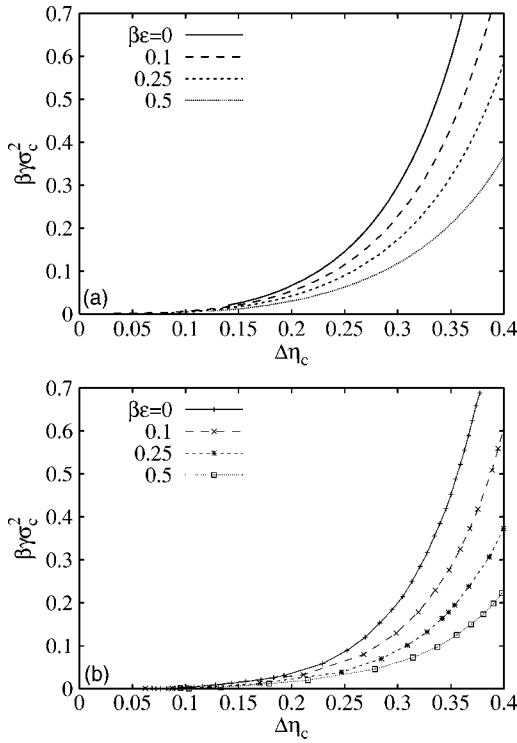


FIG. 4. Dimensionless interfacial tension, $\beta\gamma\sigma_c^2$, of the free colloidal gas-liquid interface as a function of the difference in colloid packing fractions of the coexisting states, $\Delta\eta_c = \eta_c^l - \eta_c^g$. The size ratio is $q=0.8$, and the strength of the polymer-polymer repulsion equals $\beta\epsilon=0, 0.1, 0.25$, and 0.5 as indicated. (a) DFT results; (b) simulation results.

shift of the binodal to larger values of $\beta\mu_p$ is induced by increasing $\beta\epsilon$. This seems reasonable as large values of the chemical potential are required to overcome the polymer-polymer repulsion and hence to achieve sufficiently high polymer densities that lead to phase separation.

In Fig. 4, we show results for the (scaled) gas-liquid interfacial tension, $\beta\gamma\sigma_c^2$, plotted as a function of the difference between the colloid packing fraction in the coexisting phases, $\Delta\eta_c = \eta_c^l - \eta_c^g$. Both DFT and simulation indicate that the interfacial tension decreases markedly upon increasing $\beta\epsilon$, in accordance with results from square-gradient treatment [42,43] and perturbative DFT [44]. Note that this change is not due to interfacial contributions alone, but also to the pronounced changes in the location of the bulk demixing binodal discussed above. The decrease might seem reasonable based on the profound increase in the density of the coexisting liquid upon increasing $\beta\epsilon$, see again the phase diagram in the reservoir representation, Fig. 2. As is apparent, a given value of $\Delta\eta_c$ corresponds to a reduction of η_p^r at coexistence upon increasing $\beta\epsilon$. We believe that this decrease induces the observed decrease in interfacial tension.

Alternatively, comparing the interfacial tension as a function of η_p^r thus reveals an *increase* with increasing $\beta\epsilon$; see the upper panel of Fig. 5 which shows the DFT result. The lower panel of Fig. 5 shows the corresponding simulation data. The increase in the interfacial tension with increasing $\beta\epsilon$ is confirmed up to $\beta\epsilon=0.25$, but not for $\beta\epsilon=0.5$. The simulation data for the latter case, however, should be treated

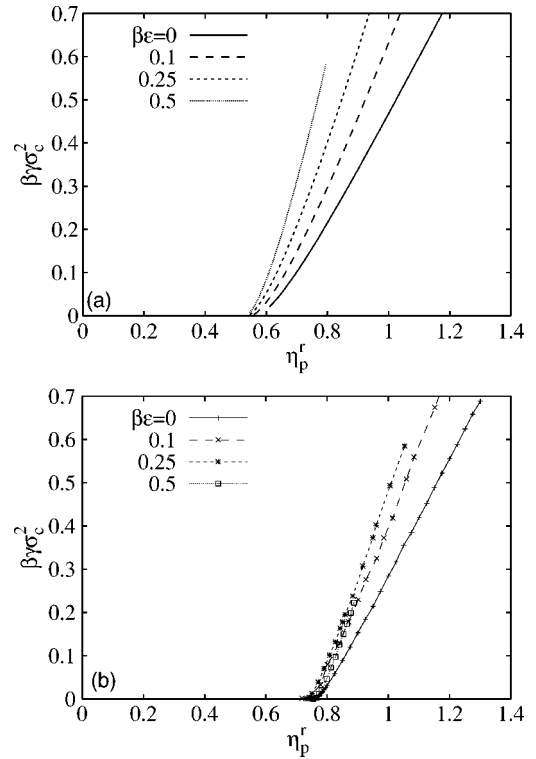


FIG. 5. The analog of Fig. 4, but as a function of the colloid packing fraction, η_c , and polymer reservoir packing fraction, η_p^r . (a) DFT results; (b) simulation results.

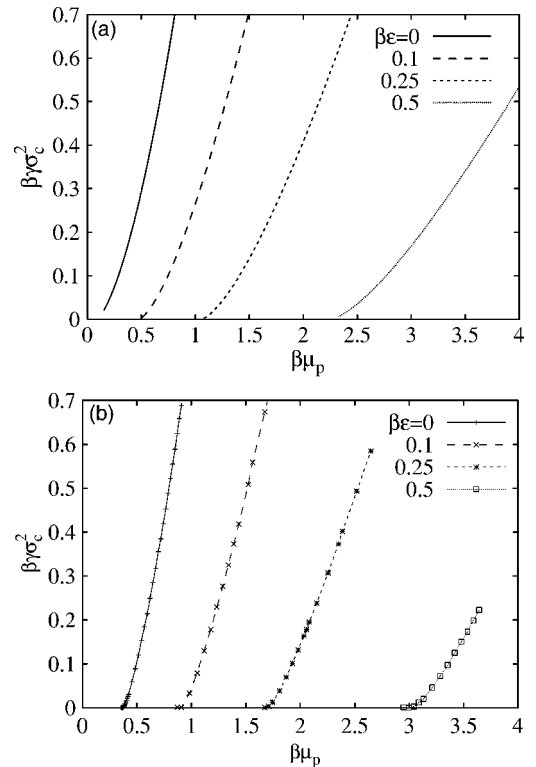


FIG. 6. The same as Fig. 4, but as a function of the (scaled) polymer chemical potential, $\beta\mu_p = \ln(z_p\sigma_p^3)$. (a) DFT results; (b) simulation results.

with some care, as in grand canonical simulations, the quantity η_p^r does not play the role of a direct control parameter, which rather the polymer fugacity, z_p , does. Consequently, conversion to the reservoir representation requires an additional step, namely the determination of η_p^r as a function of z_p . With the exception of $\beta\epsilon=0$, in which case $\eta_p^r = \pi\sigma_p^3 z_p / 6$ holds trivially, this conversion introduces an additional statistical uncertainty. Figure 2 shows that, for $\beta\epsilon=0.5$, the binodal has become very flat, so even small uncertainties in η_p^r imply rather large uncertainties in $\Delta\eta_c$. Hence, for very flat binodals, the reservoir representation is not convenient in simulations (more reliable in this case is the system representation, see Fig. 4, which, as a benefit, is experimentally more relevant). A second point is that the Monte Carlo cluster move becomes less efficient with increasing η_c and $\beta\epsilon$ (see Ref. [7]) and this will also adversely affect the data (especially for $\beta\epsilon=0.5$, since then both $\beta\epsilon$ and η_c^l are substantial). Therefore, we conclude that the shift of the simulation data for $\beta\epsilon=0.5$ in Fig. 5 most likely reflects a simulation artifact. When plotted as a function of the (scaled) chemical potential of polymers, $\beta\mu_p$, the interfacial tension shifts to significantly higher values of $\beta\mu_p$ upon increasing $\beta\epsilon$; see Fig. 6. Again this reflects the need to increase the polymer chemical potential to induce phase separation.

V. CONCLUSIONS

In conclusion, we have investigated the effect of polymer-polymer repulsion on the fluid-fluid demixing phase behavior and on the (colloidal) liquid-gas interface of a model colloid-

polymer mixture. We have used a simplistic pair potential between polymers, given by a repulsive step-function, to extend the standard AOV model to cases of interacting polymers. Grand canonical Monte Carlo simulations of the full mixture demonstrate the reasonable accuracy of the theory, with a tendency to quantitatively underestimate the shifts in the bulk fluid-fluid demixing binodal, and the gas-liquid interfacial tension, upon increasing strength of the polymer-polymer repulsion. The present study demonstrates the usefulness of the model as such, as it clearly displays previously found features due to polymer non-ideality. This offers ways to study further interesting inhomogeneous situations, like the wetting properties at substrates. Such investigations could test the robustness of the results obtained for the surface phase behavior at a hard wall using ideal polymers [9,16–19].

ACKNOWLEDGMENTS

We thank Jürgen Horbach, Marcus Müller, Kurt Binder, Marjolein Dijkstra, and Andrea Fortini for many useful and inspiring discussions. The work of M.S. is part of the research program of the *Stichting voor Fundamenteel Onderzoek der Materie* (FOM), which is financially supported by the *Nederlandse Organisatie voor Wetenschappelijk Onderzoek* (NWO). Support is acknowledged by the SFB-TR6 “Physics of colloidal dispersions in external fields” of the *Deutsche Forschungsgemeinschaft* (DFG). R.L.C. also acknowledges generous allocation of computer time on the JUMP at the Forschungszentrum Jülich GmbH.

-
- [1] W. C. K. Poon, *J. Phys.: Condens. Matter* **14**, R859 (2002).
 - [2] R. Tuinier, J. Rieger, and C. G. de Kruijff, *Adv. Colloid Interface Sci.* **103**, 1 (2003).
 - [3] S. Asakura and F. Oosawa, *J. Chem. Phys.* **22**, 1255 (1954).
 - [4] A. Vrij, *Pure Appl. Chem.* **48**, 471 (1976).
 - [5] E. J. Meijer and D. Frenkel, *J. Chem. Phys.* **100**, 6873 (1994).
 - [6] M. Dijkstra, J. M. Brader, and R. Evans, *J. Phys.: Condens. Matter* **11**, 10079 (1999).
 - [7] R. L. C. Vink and J. Horbach, *J. Chem. Phys.* **121**, 3253 (2004).
 - [8] P. G. Bolhuis, A. A. Louis, and J. P. Hansen, *Phys. Rev. Lett.* **89**, 128302 (2002).
 - [9] M. Dijkstra and R. van Roij, *Phys. Rev. Lett.* **89**, 208303 (2002).
 - [10] A. P. Gast, C. K. Hall, and W. B. Russell, *J. Colloid Interface Sci.* **96**, 251 (1983).
 - [11] H. N. W. Lekkerkerker, W. C. K. Poon, P. N. Pusey, A. Stroobants, and P. B. Warren, *Europhys. Lett.* **20**, 559 (1992).
 - [12] M. Schmidt, H. Löwen, J. M. Brader, and R. Evans, *Phys. Rev. Lett.* **85**, 1934 (2000).
 - [13] M. Schmidt, H. Löwen, J. M. Brader, and R. Evans, *J. Phys.: Condens. Matter* **14**, 9353 (2002).
 - [14] J. M. Brader and R. Evans, *Europhys. Lett.* **49**, 678 (2000).
 - [15] J. M. Brader, M. Dijkstra, and R. Evans, *Phys. Rev. E* **63**, 041405 (2001).
 - [16] J. M. Brader, R. Evans, M. Schmidt, and H. Löwen, *J. Phys.: Condens. Matter* **14**, L1 (2002).
 - [17] J. M. Brader, R. Evans, and M. Schmidt, *Mol. Phys.* **101**, 3349 (2003).
 - [18] P. P. F. Wessels, M. Schmidt, and H. Löwen, *J. Phys.: Condens. Matter* **16**, S4169 (2004).
 - [19] P. P. F. Wessels, M. Schmidt, and H. Löwen, *J. Phys.: Condens. Matter* **16**, L1 (2004).
 - [20] A. Jusufi, J. Dzubiella, C. N. Likos, C. von Ferber, and H. Löwen, *J. Chem. Phys.* **116**, 9518 (2002).
 - [21] J. Dzubiella, C. N. Likos, and H. Löwen, *J. Chem. Phys.* **116**, 9518 (2002).
 - [22] B. Rotenberg, J. Dzubiella, A. A. Louis, and J. P. Hansen, *Mol. Phys.* **102**, 1 (2004).
 - [23] P. B. Warren, S. M. Ilett, and W. C. K. Poon, *Phys. Rev. E* **52**, 5205 (1995).
 - [24] W. C. K. Poon, J. S. Selfe, M. B. Robertson, S. M. Ilett, A. D. Priorie, and P. N. Pusey, *J. Phys. II* **3**, 1075 (1993).
 - [25] M. Schmidt, A. R. Denton, and J. M. Brader, *J. Chem. Phys.* **118**, 1541 (2003).
 - [26] P. G. Bolhuis, A. A. Louis, J. P. Hansen, and E. J. Meijer, *J. Chem. Phys.* **114**, 4296 (2001).
 - [27] Y. Rosenfeld, *Phys. Rev. Lett.* **63**, 980 (1989).
 - [28] R. Evans, *Adv. Phys.* **28**, 143 (1979).
 - [29] R. Evans, in *Fundamentals of Inhomogeneous Fluids*, edited

- by D. Henderson (Dekker, New York, 1992), Chap. 3, p. 85.
- [30] S. M. Ilett, A. Orrock, W. C. K. Poon, and P. N. Pusey, *Phys. Rev. E* **51**, 1344 (1995).
- [31] M. Schmidt, M. Dijkstra, and J. P. Hansen, *Phys. Rev. Lett.* **93**, 088303 (2004).
- [32] A. Z. Panagiotopoulos, *Mol. Phys.* **61**, 813 (1987).
- [33] P. Virnau and M. Müller, *J. Chem. Phys.* **120**, 10925 (2003).
- [34] K. Binder, *Phys. Rev. A* **25**, 1699 (1982).
- [35] R. L. C. Vink, J. Horbach, and K. Binder, *Phys. Rev. E* **71**, 011401 (2005).
- [36] E. H. A. de Hoog and H. N. W. Lekkerkerker, *J. Phys. Chem. B* **103**, 5274 (1999).
- [37] E. H. A. de Hoog and H. N. W. Lekkerkerker, *J. Phys. Chem. B* **105**, 11636 (2001).
- [38] D. G. A. L. Aarts, J. H. van der Wiel, and H. N. W. Lekkerkerker, *J. Phys.: Condens. Matter* **15**, S245 (2003).
- [39] D. G. A. L. Aarts, M. Schmidt, and H. N. W. Lekkerkerker, *Science* **304**, 847 (2004).
- [40] A. Vrij, *Physica A* **235**, 120 (1997).
- [41] A. Fortini, M. Dijkstra, M. Schmidt, and P. P. F. Wessels, *Phys. Rev. E* **71**, 051403 (2005).
- [42] D. G. A. L. Aarts, R. P. A. Dullens, H. N. W. Lekkerkerker, D. Bonn, and R. van Roij, *J. Chem. Phys.* **120**, 1973 (2004).
- [43] A. Moncho-Jordá, B. Rotenberg, and A. A. Louis, *J. Chem. Phys.* **119**, 12667 (2003).
- [44] A. Moncho-Jordá, J. Dzubiella, J. P. Hansen, and A. A. Louis, *J. Phys. Chem. B* **109**, 6640 (2005).
- [45] D. G. A. L. Aarts, R. Tuinier, and H. N. W. Lekkerkerker, *J. Phys.: Condens. Matter* **14**, 7551 (2002).
- [46] A. A. Louis, P. G. Bolhuis, E. J. Meijer, and J. P. Hansen, *J. Chem. Phys.* **117**, 1893 (2002).
- [47] M. Schmidt, A. Fortini, and M. Dijkstra, *J. Phys.: Condens. Matter* **48**, S3411 (2003).
- [48] M. Schmidt, A. Fortini, and M. Dijkstra, *J. Phys.: Condens. Matter* **16**, S4159 (2004).
- [49] D. G. A. L. Aarts and H. N. W. Lekkerkerker, *J. Phys.: Condens. Matter* **16**, S4231 (2004).
- [50] R. Evans and U. Marini Bettolo Marconi, *J. Chem. Phys.* **86**, 7138 (1987).
- [51] R. L. C. Vink, J. Horbach, and K. Binder, *J. Chem. Phys.* **122**, 134905 (2005).
- [52] M. Schmidt, *J. Phys.: Condens. Matter* **11**, 10163 (1999).
- [53] R. L. C. Vink, in *Computer Simulation Studies in Condensed Matter Physics XVIII*, edited by D. P. Landau, S. P. Lewis, and H. B. Schuettler (Springer, Berlin, 2004).
- [54] R. L. C. Vink and J. Horbach, *J. Phys.: Condens. Matter* **16**, S3807 (2004).
- [55] M. Müller and N. B. Wilding, *Phys. Rev. E* **51**, 2079 (1995).
- [56] L. G. MacDowell, P. Virnau, M. Müller, and K. Binder, *J. Chem. Phys.* **120**, 5293 (2004).
- [57] P. Virnau, L. G. MacDowell, M. Müller, and K. Binder, in *High Performance Computing in Science and Engineering 2004*, edited by S. Wagner, W. Hanke, A. Bode, and F. Durst (Springer, Berlin, 2004), p. 125.
- [58] K. Binder, *Z. Phys. B* **43**, 119 (1981).
- [59] A. D. Bruce and N. B. Wilding, *Phys. Rev. Lett.* **68**, 193 (1992).
- [60] Y. C. Kim, M. E. Fisher, and E. Luijten, *Phys. Rev. Lett.* **91**, 065701 (2003).